Nanoferrites as Catalysts and Fillers for Polyaniline/Nanoparticle Composites Preparation

E. Falletta[1], A. Ponti[2], A. Sironi[1], A. M. Ferretti[2] and C. Della Pina[1,*]

[1]*Dipartimento di Chimica, Università degli Studi di Milano, CNR-ISTM, via Golgi, 19, 20133, Milano, Italy*

[2]*Laboratorio di Nanotecnologie, Istituto di Scienze e Tecnologie Molecolari, Consiglio Nazionale delle Ricerche, Via G. Fantoli, 16/15-20138-Milan Italy*

Abstract: In this paper, we report on the catalytic activity of MFe_2O_4 nanoparticles (M = Mn, Ni, Cu, Zn, Mg) in the oxidative polymerization of *N*-(4-aminophenyl)aniline yielding polyaniline/nanoparticle composites. Hydrogen peroxide is used as the oxidizing agent and ferrite nanoparticles play the dual role of reaction catalysts and fillers. The obtained polyaniline/MFe_2O_4 composites maintained the pristine size of the ferrite crystallites and showed a modest conductive behavior. Polyaniline/MFe_2O_4 (M = Mn, Ni) composites displayed good dispersion of the nanoparticles in the polyaniline matrix and magnetic hardness intermediate between those of soft M = Fe and hard M = Co composites, evidencing the tunability of the magnetic properties.

Keywords: Catalysis, Composites, Ferrites, Nanoparticles, Polyaniline.

INTRODUCTION

Materials having both electrical and magnetic properties have attracted much interest thanks to their features combining the advantages of inorganic materials (mechanical strength, electrical and magnetic properties, as well as thermal stability) with those of organic compounds (flexibility, ductility and processing) [1]. Among them, intrinsically conducting polymers (ICPs) containing magnetic nanoparticles (NPs) exhibit many potential applications in electromagnetic interference shielding, [2] electrochromic devices [3] and non-linear optical systems [4]. Polyaniline (PANI) is one of the most investigated ICPs thanks to its extraordinary electrical properties, reversibly switching from an insulator to a conducting material by deprotonation/protonation processes [5, 6]. It can exist in different forms: leucoemeraldine (totally reduced form, x = 1 in Figure **1**), emeraldine (half-oxidized form, x = 0.5 in Figure **1**), pernigraniline (totally oxidized form, x = 0 in Figure **1**) and many other intermediate structures (Figure **1**).
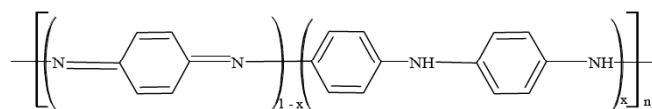

Figure 1: Polyaniline structures.

PANI/NPs composites are typically prepared by multi-step approaches involving NPs synthes is followed by aniline polymerization. The inorganic particles can be embedded during the polymerization process or in a subsequent step [7-10].

Inspired by our experience in the field of catalysis [11-13] and in the preparation of conducting polymers by innovative eco-friendly approaches, [14-16] we recently reported a new method to produce electrical and magnetic polyaniline nanocomposites, (PANI)/Fe_3O_4 and PANI/$CoFe_2O_4$, where the magnetic nanoparticles played the dual role of catalysts and magnetic fillers [17, 18].

In order to extend this study to PANI nanocomposites with different nanoferrites, we investigated the catalytic properties of nanosized MFe_2O_4, where M was Mn, Ni, Cu, Zn, and Mg, in the *N*-(4-aminophenyl)aniline oxidative polymerization to obtain electrical and magnetic PANI/MFe_2O_4 nanocomposites.

EXPERIMENTAL

All chemicals were purchased by Sigma Aldrich and used as received without further purification. FT-IR spectra (500-4000 cm^{-1}) were recorded by a JASCO FT/IR-410 spectrophotometer. The NPs morphology study was performed by transmission electron microscopy (TEM) using a Zeiss LIBRA-200FE microscope; the specimen were preparing by drop casting a dispersion of NPs or nanocomposite suspension in acetonitrile on a 5 nm carbon-film copper grid. TEM images were processed by means of a Imaging Platform software (Olympus). The metal content of all materials was determined by atomic

*Address correspondence to this author at the Dipartimento di Chimica, Università degli Studi di Milano, CNR-ISTM, via Golgi, 19, 20133, Milano, Italy; Tel: +39 0250314410; Fax: +39 02 50314405; E-mail: cristina.dellapina@unimi.it

absorption analysis on a AAnalyst3100 PerkinElmer spectrophotometer after sample mineralization in aqua regia. A Quantum Design MPMS XL-5 SQUID magnetometer was used to measure the magnetization isotherm of the nanoferrite samples between +50 and – 50 kOe at 5 K. All the data were corrected for sample holder diamagnetic contribution. The dia-, para and superpara-magnetic contributions of the nanoferrite to the magnetization isotherm were identified by the method proposed by Fabian [19].

Powder X-ray diffraction (XRD) patterns were recorded using a Rigaku D IIIMAX horizontal-scan powder diffractometer with Cu Kα radiation.

For conductivity measurements, 200 mg of finely powdered samples were pressed between 13 mm anvils with force 10 ton for 30 min. Each pellet was subjected to 2 kg weight. After 30 min, the resistance R was measured by an AMEL338 multimeter and conductivity σ was obtained by the following equation:

$$\sigma = (1/R) \, (\ell/A)$$

where ℓ is the thickness of the disk and A is the area of the disk base.

MFe$_2$O$_4$ NANOPARTICLES (NPs) PREPARATION

All MFe$_2$O$_4$ NPs were prepared according to a method reported in the literature [20]. Briefly, a solution of FeCl$_3\cdot$6H$_2$O ([Fe^{+3}] = 0.30 M, solution A) and a solution of MCl$_2\cdot$xH$_2$O ([M^{+2}] = 0.15 M, solution B), where M was Mn, Co, Ni, Mg and Zn, were prepared dissolving the appropriate amount of salts in 10 mL of 0.4 M HCl, always maintaining the atomic ratio Fe/M= 2. The two solutions were mixed and stirred at 80°C under inert atmosphere for 20 min. Then, an aqueous solution of 1.5 M NaOH was quickly added until reaching pH 13 and the mixture was maintained under vigorous stirring for 2 h. Finally, a dark brown product was magnetically decanted, washed several times with deionized water until neutral pH of the liquor mothers and dried at 70°C in oven.
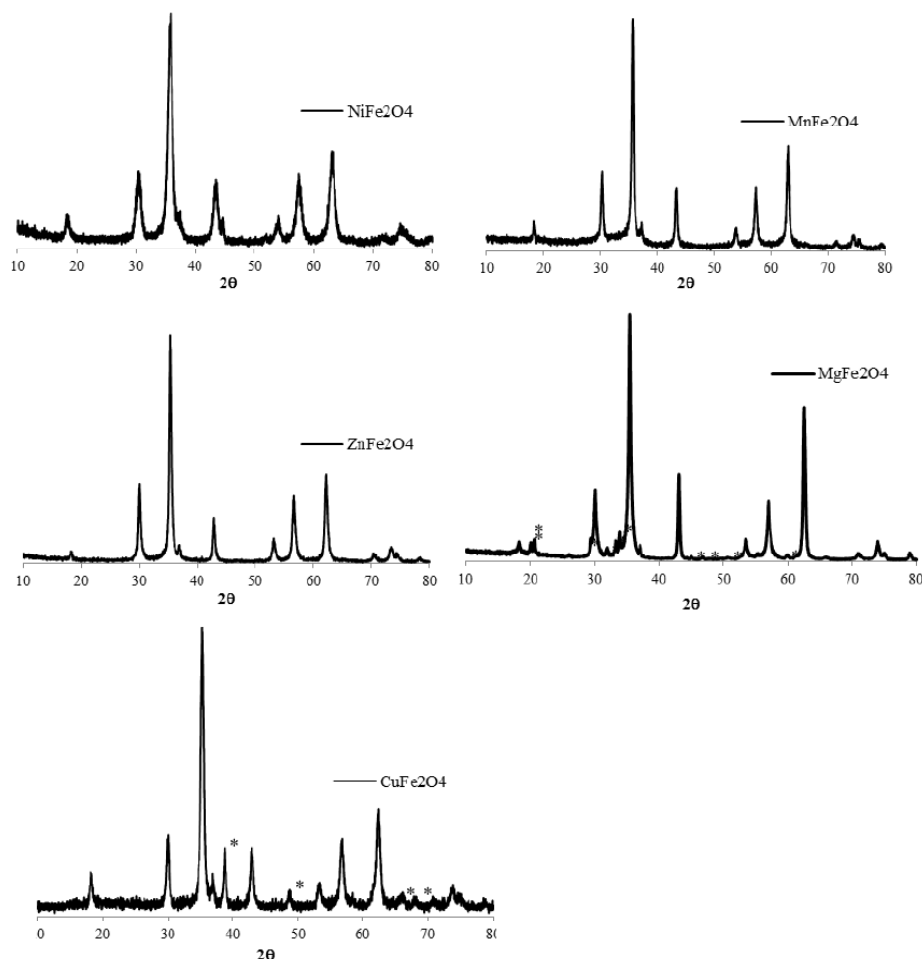

Figure 2: XRPD patterns of MFe$_2$O$_4$ nanoferrites.

SYNTHESIS OF PANI/NPs COMPOSITES

500 mg of *N*-(4-aminophenyl)aniline (aniline dimer, AD) were dissolved in 90 mL of 0.03 M HCl. Then, 1.4 mL of H_2O_2 (30% w/w; H_2O_2/AD=5 molar ratio) were added quickly followed by a proper amount of powdered MFe_2O_4NPs (AD/MFe_2O_4= 5 molar ratio). The mixture was stirred at room temperature for 24 h. Finally, the reaction was stopped by the addition of acetone. After 20 min a dark solid was recovered by filtration, washed several times with deionized water and acetone until the mother liquor resulted to be colorless and finally dried in an oven (80°C) for 6 h.

The reaction was repeated in the absence of MNPs and, as reported in our previous work [16], a green solid material was obtained with 36% yield.

RESULTS AND DISCUSSION

Characterization of MFe_2O_4 Nanoparticles

All MFe_2O_4NPs were characterized by XRP diffraction and the results are reported in Figure **2**.

These diffractograms show that all NPs have the cubic ferrite (spinel) structure [21-24]. The XRPD pattern of M = Mn, Ni, Zn NP batches closely match the ferrite pattern showing that these comprise a pure ferrite phase, whereas those of $CuFe_2O_4$ and $MgFe_2O_4$ display additional peaks (*) that can be assigned to CuO in the case of $CuFe_2O_4$. The additional peaks displayed in $MgFe_2O_4$ pattern could not be identified despite extensive database search (diffrac.eva program).

The average diameters of MFe_2O_4 NPs, as deter-mined by the Scherrer equation, and Fe/M atomic ratios, as measured by AAS, are summarized in Table **1**.

Table 1: Mean Diameter (by XRPD) and Fe/M Atomic Ratio of MFe_2O_4 NPs (by AAS)

Ferrite NPs	Mean d (nm)	Fe/M (Atomic Ratio)
$MnFe_2O_4$	19.0	2.3
$NiFe_2O_4$	10.6	2.1
$CuFe_2O_4$	15.4	2.1
$ZnFe_2O_4$	18.4	1.8
$MgFe_2O_4$	19.3	1.9

NPs were obtained with similar mean diameters and Fe/M atomic ratios in good agreement with the stoichiometric value (Fe/M = 2).

TEM images of NPs show that all the samples are morphologically polydispersed and their spinel structure is confirmed by electron diffraction (ED) patterns (Figure **3**).Table **2** summarizes the values of median, minimum and maximum diameter and standard deviation for all MFe_2O_4 NPs as extracted by TEM images, except for $MgFe_2O_4$. In this latter case, diameters could not be reliably measured because the sample was largely aggregated, though single nanoparticles were visible. The results obtained for M = Mn, Ni are in agreement with the XRD achievements (Table **1**), thereby indicating that in this case NPs are monocrystalline. On the other hand, the size of $CuFe_2O_4$ NPs measured by TEM is slightly larger than that calculated from XRPD patterns by the Scherrer equation, thus suggesting a possible polycrystalline structure. Similarly, for $ZnFe_2O_4$ NPs the large difference between XRPD and TEM size is firm evidence that these NPs are polycristalline.

Table 2: Median (Med d), Maximum (Max d), and Minimum (Min d) Diameter, and Standard Deviation (Std Dev) of MFe_2O_4 NPs as Estimated from TEM Images

Ferrite NPs	Med d (nm)	Std Dev(nm)	Min d (nm)	Max d (nm)
$MnFe_2O_4$	15.5	5.8	7.1	33.1
$NiFe_2O_4$	9.4	3.0	2.8	22.1
$CuFe_2O_4$	21.6	not estimated	10.5	45.1
$ZnFe_2O_4$	91.6	not estimated	8.9	33.7

Catalytic Polymerization

Polyaniline can be produced following many different methods including chemical, electrochemical and enzymatic approaches [25]. Aniline polymerization by means of oxidants in stoichiometric amount is the oldest and still the most used procedure, although it involves serious drawbacks: toxic oxidants use, plenty of inorganic co-products and carcinogenic intermediates production (*e.g.*, benzidine).

It was observed that the necessity to employ strong oxidizing agents in large amount is related to thermodynamic limitations [26, 27], consisting in the oxidation of aniline monomer to form dimeric species representing the most energy-demanding step of polymerization.

As we recently demonstrated, when *N*-(4-aminophenyl)aniline (aniline dimer, AD), a commercially available material, [28] is used as the starting reagent, hard oxidants can be replaced by
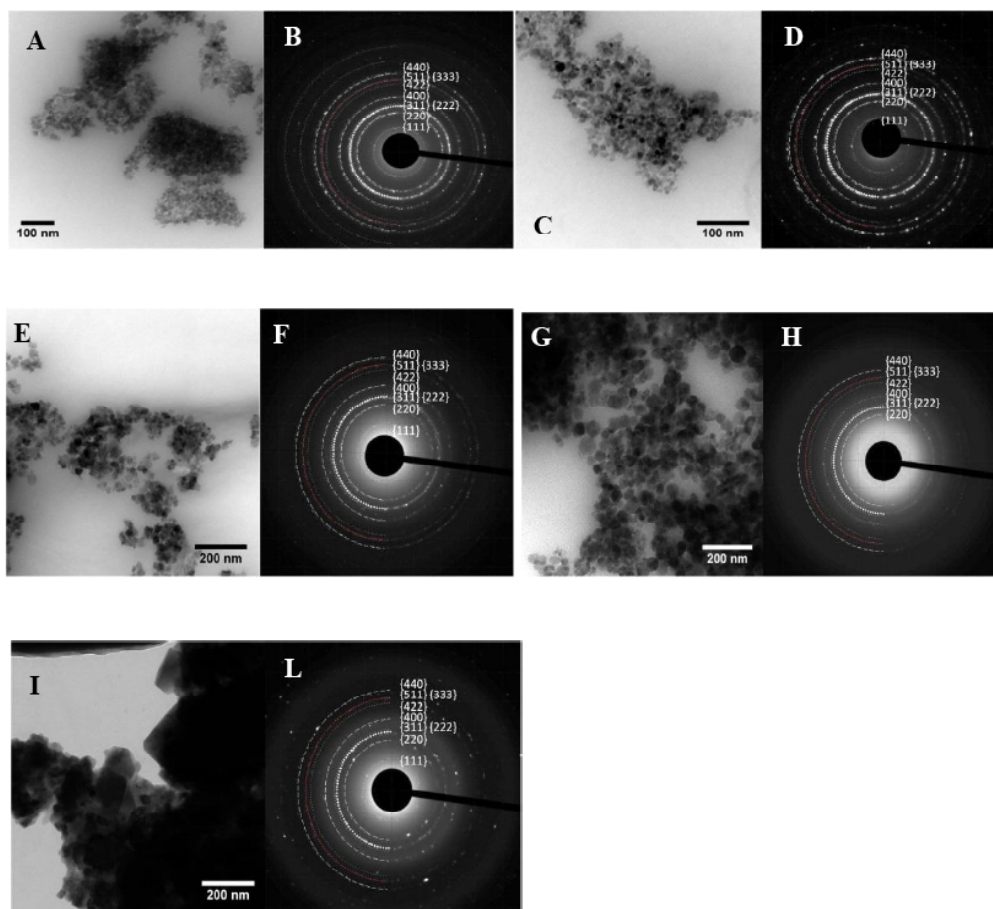
Figure 3: TEM images of MnFe$_2$O$_4$ (A), NiFe$_2$O$_4$ (C), CuFe2O4 (E), ZnFe2O4 (G) and MgFe2O4 (I) NPs (scale bar = 100 nm and 200 nm) and the corresponding electron diffraction patterns (**B, D, F, H** and **L**).

greener ones (molecular oxygen or hydrogen peroxide) in the oxidative polymerization reaction with the aid of proper catalysts [16-18]. On this regard, MFe$_2$O$_4$- prepared as described in section Experimental- were employed both as the catalysts and (magnetic) fillers for the preparation of PANI/MFe$_2$O$_4$nanocomposites. Figure **4** displays the yield values as calculated according to Eq. (1):

Figure 4: Dependence of the yield of PANI/MFe$_2$O$_4$ composite on the MFe2O4/AD molar ratio.

$$\text{Yield \%} = [\Sigma_{(\text{mass of insoluble product})}/\Sigma_{(\text{mass reagents})}] \times 100 \qquad (1)$$

As featured in our previous work [16], in the absence of any catalyst *N*-(4-aminophenyl)aniline oxidative polymerization proceeded leading to polyaniline with 36% yield. Therefore, this value should be subtracted from the results reported in Figure **4** to evaluate the real catalytic activity of the NPs. When compared to the achievements observed using Fe$_3$O$_4$ and CoFe$_2$O$_4$ as the catalysts [17, 18], the NPs show a similar catalytic behaviour increasing with the MFe$_2$O$_4$ amount, up to reaching polymerization yields between 70 and 80%. However, some differences are evident. On one hand, at low MFe$_2$O$_4$/AD molar ratio (0.01), MnFe$_2$O$_4$ and ZnFe$_2$O$_4$ NPs led to reaction yields close to that obtained in the absence of any catalyst, on the other hand, all the other nanoferrites (M = Ni, Cu, Mg) seem to suppress the spontaneous ability of H$_2$O$_2$ to polymerize AD. Moreover, for all the MFe$_2$O$_4$/AD molar ratios investigated, the catalytic activity of these NPs always remained lower than that registered for MnFe$_2$O$_4$ and ZnFe$_2$O$_4$ NPs. Regarding NiFe$_2$O$_4$ NPs,
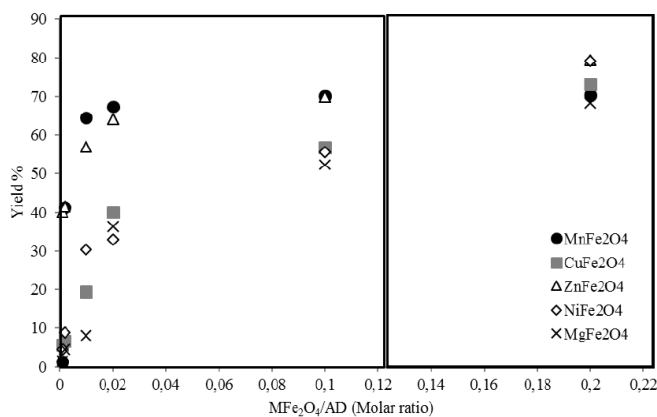
an irregular behaviour was registered. Accordingly, on the left side of Figure **4** (low MFe_2O_4/AD molar ratios) Ni-ferrites exhibited similar catalytic activity as those of Cu- and Mg-ferrites, whereas at high MFe_2O_4/AD ratios, they were able to reach the catalytic performances of Mn- and Zn-ferrite NPs. These unexpected results could be connected to different reasons. First of all, the presence of impurities (probably, single metal oxides M_xO_y) in some NPs could negatively affect their catalytic activity towards *N*-(4-aminophenyl)aniline oxidative polymerization. This inhibitory effect seems to prevail at low MFe_2O_4/AD molar ratios, whereas increasing the amount of NPs in the reaction mixture and, as a consequence, of Fe^{+3} sites, all the ferrites recovered their catalytic ability. However, if on the one hand the presence of inorganic impurities in nano-ferrites could justify the low catalytic performances of $CuFe_2O_4$ and $MgFe_2O_4$ NPs, on the other hand this explanation fails in the attempt to interpret the $NiFe_2O_4$ NPs catalytic behaviour, because these NPs were free from impurities. A second possible reason that might disentangle the different catalytic behaviour could be related to the heterogeneous Fenton-like activity of ferrites, as recently demonstrated by He *et al*. [29]. The authors compared the different ability of MFe_2O_4 materials (where M was Ti, Cr, Mn, Co and Ni) to generate ·OH radicals. Even though various mechanisms have been proposed for explaining polyaniline formation, most of them agrees to consider that radicals play a key role [30-32]. The higher ability of $MnFe_2O_4$ and $CoFe_2O_4$NPs to produce

·OH radicals than $NiFe_2O_4$ NPs seems to reflect our results. In fact, manganese ferrite allowed the highest activity in the catalytic *N*-(4-aminophenyl)aniline oxidative polymerization, as well as cobalt ferrite, as previously demonstrated [18].

PANI/NPs Composites Characterization

RegardingPANI/NPs composites, FT-IR analyses revealed the polymeric matrix (polyaniline) to be in its conducting emeraldine form, as shown by the similar intensity of the two bands at 1498 cm^{-1} and 1484 cm^{-1} assigned to the C=C stretching vibration modes of the quinoid and benzenoid groups, respectively, and by the strong electronic-like band at around 1144 cm^{-1} (Figure **5**) [33].

Concerning XRPD patterns of PANI/NPs composite, it was possible to distinguish the broad peak at around 25°, assigned to amorphous polyaniline, as well as the presence of all the spinel diffraction peaks of nanoferrites discussed above (Figure **6**). Moreover, the diffraction peaks of impurities observed in the diffractograms of $CuFe_2O_4$ and $MgFe_2O_4$ NPs (Figure **2**) were not evident in the XRPD patterns of composites, showing that the impurities were not embedded in the composites and, therefore, did not impact the composite properties. As reported in Table **3**, it is evident that the mean diameter of the nanocrystals (as opposed to NPs), embedded in the composite, are close to those of pristine ferrites. Thus,
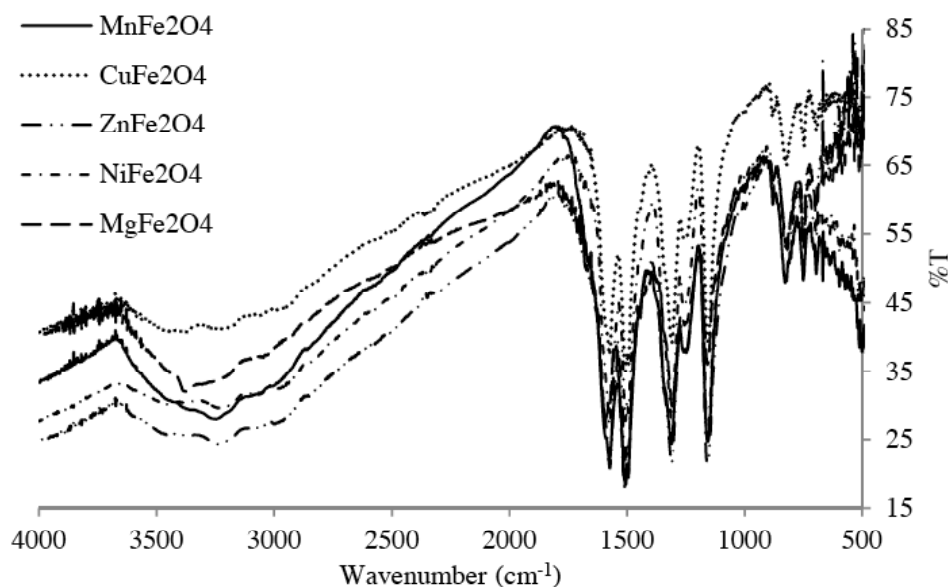

Figure 5: FT-IR spectra of PANI/MFe_2O_4 composites obtained using a MFe_2O_4/AD molar ratio of 0.2.

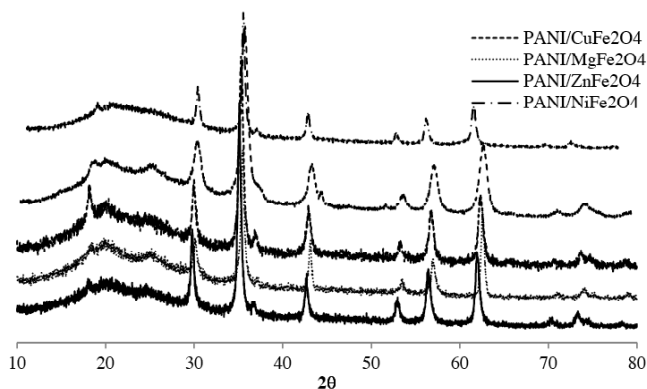the polymerization reaction environment did not affect the ferrite crystal size.

Figure 6: XRPD patterns of PANI/NPs composites obtained using a MFe_2O_4/AD molar ratio of 0.20.

Table 3: **Mean Diameter (by XRPD), Fe/M Atomic Ratio and MFe_2O_4 Content in Composites Obtained using the MFe_2O_4/AD Molar Ratio of 0.20. *Theoretical Values**

Sample	Mean d (nm)	Fe/M (atomic ratio)	MFe_2O_4/composite (%w/w)
PANI/MnFe$_2$O$_4$	17.9	2.0	23.9 (25.0)*
PANI/NiFe$_2$O$_4$	10.4	2.3	18.9 (22.2)*
PANI/CuFe$_2$O$_4$	15.6	2.8	20.9 (24.6)*
PANI/ZnFe$_2$O$_4$	18.9	2.0	21.3 (22.6)*
PANI/MgFe$_2$O$_4$	17.6	3.0	17.2 (24.2)*

As far as the Fe/M atomic ratio is concerned, if on the one hand the achievements for $MnFe_2O_4$, $NiFe_2O_4$ and $ZnFe_2O_4$ NPs were in good agreement with the stoichiometric value (Fe/M = 2), on the other hand for $MgFe_2O_4$ and $CuFe_2O_4$ it resulted to be higher than 2. The loss of metal M suggests that the impurities observed in the case of $MgFe_2O_4$ and $CuFe_2O_4$

patterns (Figure **2**) probably consist of M-containing oxides (or other species) which might dissolve in the reaction mixture during the polymerization reaction.

Likewise, atomic absorption spectroscopy showed that $MnFe_2O_4$ and $ZnFe_2O_4$ NPs were completely embedded in the polymeric matrix (MFe_2O_4 loss $\cong$ 1%), whereas the amount of embedded $NiFe_2O_4$, $CuFe_2O_4$, and $MgFe_2O_4$ NPs was lower than the expected value by 3, 4, and 7%, respectively.

All these observations confirm the hypothesis that $MnFe_2O_4$ and $ZnFe_2O_4$ NPs acted as heterogeneous Fenton-like catalysts in the AD oxidative polymerization reaction, as well as their high catalytic activity was not related to their partial corrosion in the reaction mixture. Furthermore, the impurities present in $MgFe_2O_4$ and $CuFe_2O_4$ NP batches inhibited the ability of MFe_2O_4 to catalyse the polymerization reaction, although not embedded in the composite. $NiFe_2O_4$ NPs again displayed an intermediate character. As a general trend, by increasing the MFe_2O_4/AD molar ratio, the ferrite catalytic activity always prevailed.

Since $MnFe_2O_4$ and $NiFe_2O_4$ NPs displayed the highest and medium catalytic activity in the AD oxidative polymerization, the corresponding composites were selected for TEM and magnetic investigations.

TEM images of PANI/MFe_2O_4 (M = Mn, Ni) composites, obtained using a MFe_2O_4/AD molar ratio of 0.20, are reported in Figure **7**. In addition to conventional bright-field images, we also recorded images formed by collecting electrons which underwent a 30 eV energy loss by interaction with the specimen. These energy-filtered images have higher contrast between the bright organic matrix and the dark inorganic NPs. The TEM images show that the NPs are well dispersed in the polymeric matrix and their morphology did not significantly changed. Electron diffraction patterns (not reported), confirmed that the
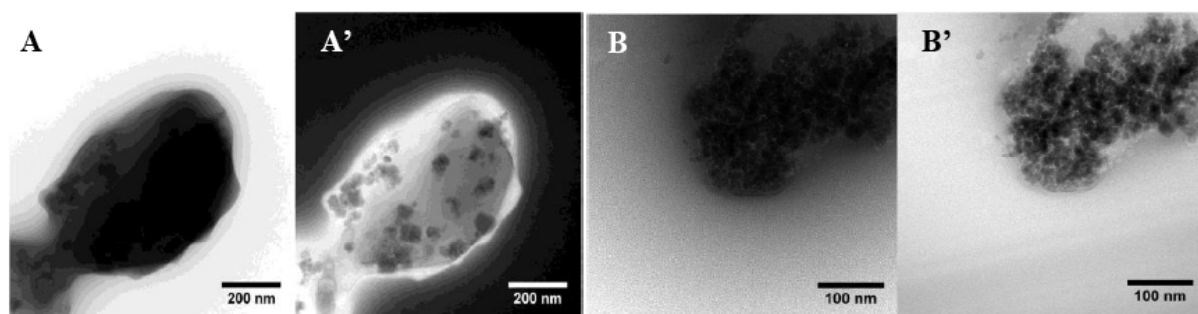

Figure 7: TEM images of PANI/$MnFe_2O_4$ (**A, A'**) and PANI/$NiFe_2O_4$ (**B, B'**) composites obtained using a MFe_2O_4/AD molar ratio of 0.20. **A** and **B** are conventional bright-field images; **A'** and **B'** were recorded collecting electrons which underwent a 30 eV energy loss.

NPs embedded in PANI matrix maintained the cubic ferrite structure.

The T = 5 K isothermal magnetization curves of PANI/MFe_2O_4 (M = Mn, Ni) composites, obtained using a MFe_2O_4/AD molar ratio of 0.20, are reported in Figure **8** and the main magnetic parameters are collected in Table **4**. The coercivity H_c is sizeable for cubic ferrites, making these composites intermediate between magnetically soft PANI/Fe_3O_4 ($H_c \approx$ 0.1 kOe) [17] and hard PANI/$CoFe_2O_4$ ($H_c \approx$ 10 kOe) [18]. The microcoercivity, i. e. the coercivity of individual NPs, is better represented by the remanence coercivity H_{cr}, which can be estimated by the ΔM method [34]. The H_{cr} data confirm the intermediate magnetic nature of these composites and a considerable contribution of reversible mechanisms to magnetization inversion at low (< 1 kOe) fields.

The saturation (M_{sat}) and remanent (M_{rem}) magnetization again indicate an intermediate behavior between soft PANI/Fe_3O_4 and hard PANI/$CoFe_2O_4$, as evidenced by the M_{rem}/M_{sat} ratio, which is *ca.* 0.1 and 0.5 for M = Fe and Co, respectively. The M_{rem}/M_{sat} ratio for the present PANI/$NiFe_2O_4$ and PANI/$MnFe_2O_4$ is lower than that expected (about 0.5) for Stoner-Wollforth NPs, indicating the significant presence of superparamagnetic NPs even at T = 5 K. The M_{sat} value of PANI/$MnFe_2O_4$, though lower than the bulk value 112 emu/g, [35] is not unexpected in ferrite

nanoparticles and usually attributed to surface effects [36]. For PANI/$NiFe_2O_4$, M_{sat} was instead found to be larger than the bulk value 56 emu/g [35]. This could be related to the Fe/Ni ratio (Table **3**) that is higher than the stoichiometric value. However, based on the bulk M_{sat} = 98 emu/g of Fe_3O_4 and the Fe/Ni = 2.3 ratio, we expected M_{sat} = 59 emu/g, that is lower than the observed one. Hence, the Fe excess is not able to fully account for the anomalously high M_{sat} of $NiFe_2O_4$.

The calculation of M_{sat} from isothermal magnetization data of NPs could be affected by the presence of NPs in the superparamagnetic regime. To improve the calculation of M_{sat}, we resorted to a method [19] based on the analysis of the approach to saturation. At high-field, the magnetization M is modeled as:

$$M(H) = M_{sat} + \chi H + \alpha H^\beta$$

where χ represents all dia- and para-magnetic contributions and the last term represents the approach to saturation. The β parameter is -2 for homogeneous magnetization rotation and -1 for superparamagnetic ensembles. By fitting the last expression to the high-field data, we obtained the best-fit parameters collected in Table **5**. The β values indicate that both ferrimagnetic (blocked) and superparamagnetic NPs contribute to the approach to saturation and the corrected M_{sat} value of PANI/$NiFe_2O_4$ is closer to the bulk value.
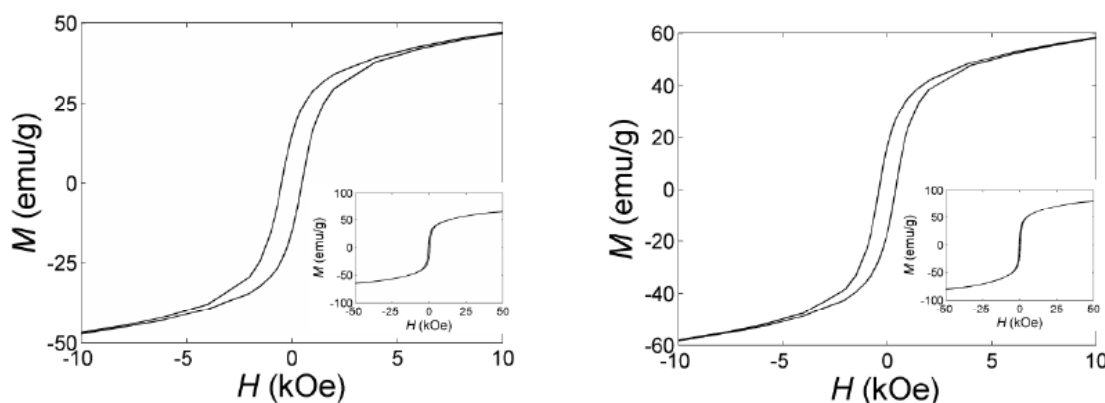

Figure 8: Isothermal magnetization curves of PANI/$NiFe_2O_4$ (left) and PANI/$MnFe_2O_4$ (right) composites, obtained using a MFe_2O_4/AD molar ratio of 0.20. The subpanels show the entire isotherm between −50 and + 50 kOe.

Table 4:   Magnetic Properties of Selected (M = Mn, Ni) PANI/MFe_2O_4 Composites Derived from Magnetization Isotherm at T = 5 K. ([a] Mass Magnetization Referred to NP Mass (*not* Composite Mass). [b]M_{sat} Actually is M (50 kOe) as this Sample is not Completely Saturated at 50 kOe. [c] Estimated using the ΔM Method [31]

M	M_{sat}[a,b](emu/g)	M_{rem}[a] (emu/g)	M_{rem}/M_{sat}	H_c (kOe)	H_{cr}[c] (kOe)	H_{cr}/H_c
Ni	64.7	15.3	0.24	0.48	0.87	1.80
Mn	80.4	16.9	0.21	0.39	0.75	1.90

Table 5: **Magnetization of selected (M = Mn, Ni) PANI/MFe$_2$O$_4$ Composites Values Corrected from Sample Dia-, Para-, and Superpara-Magnetic Contributions. [^{a} Mass Magnetization Referred to NP Mass (*not* Composite Mass). ^{b}M$_{sat}$ Actually is M(50 kOe) as Even the Blocked Part of the Sample Might not be Completely Saturated at 50 kOe]**

M	β	$M_{sat}^{a,b}$ (emu/g)	M_{rem}^{a} (emu/g)	M_{rem}/M_{sat}
Ni	−1.14	57.0	15.4	0.27
Mn	−1.12	72.2	16.9	0.23

Conductivity values of all the PANI/MFe$_2$O$_4$ composites synthesized using a MFe$_2$O$_4$/AD molar ratio of 0.2 were measured as described in the experimental part. All the materials resulted to be less conducting than traditional PANI prepared from aniline (typically 4.4 S/cm) [37] with values of conductivity between $2.0 \cdot 10^{-6}$ and $3.5 \cdot 10^{-7}$ S/cm, despite FTIR spectroscopy showed that the polymer was in the conducting emeraldine form. Although the lower conducting behaviour of the composites can be attributed to the presence of insulating nanoparticles, a real comparison among conductivity values of polyaniline prepared by different protocols and measurements recorded by various methods and under different conditions is very hard. In fact, it has been extensively demonstrated that PANI conductivity is affected by numerous factors, such as crystallinity degree, molecular weight, humidity level, branching presence, type and amount of dopants, as well as pressure applied on samples during measurements [38-40].

CONCLUSIONS

The catalytic behavior of MFe$_2$O$_4$ NPs (M = Ni, Mn, Cu, Mg and Zn) in the oxidative polymerization of *N*-(4-aminophenyl)aniline to produce PANI/MFe$_2$O$_4$ composites has been herein described. The difference in the catalytic performance of the various ferrites nanoparticles was attributed to two main factors: the purity level of the inorganic particles and their different ability to decompose H$_2$O$_2$ to ·OH radicals, involved in the polyaniline formation.

Ferrites seem to act as heterogeneous Fenton-like catalysts. More in detail, MnFe$_2$O$_4$ and ZnFe$_2$O$_4$ led to PANI in high yield, NiFe$_2$O$_4$ showed an intermediate behavior, whereas CuFe$_2$O$_4$ and MgFe$_2$O$_4$ efficiently worked only under specific conditions. All the ferrites, totally embedded in the polymeric matrix, retained their pristine crystal size as evinced by XRPD and TEM investigations. The (remanence) coercivity of PANI/NiFe$_2$O$_4$ and PANI/MnFe$_2$O$_4$ composites was found to beintermediate between those of magnetically

soft PANI/Fe$_3$O$_4$ and hard PANI/CoFe$_2$O$_4$. Hence, our approach enables effective control of the magnetic hardness of composites with comparable specific magnetization. Finally, all PANI/ferrites composites exhibited a modest conducting behavior, even though the polymeric matrix was found to correspond to PANI in its emeraldine conducting form.

ACKNOWLEDGMENTS

REFERENCES

[1]   Jiang J, Li L, Zhu M. Polyaniline/magnetic ferrite nanocomposites obtained by in situ polymerization. React FunctPolym 2008; 68(1): 57-62.
http://dx.doi.org/10.1016/j.reactfunctpolym.2007.10.010

[2]   Miyauchi S, Aiko H, Sorimashi Y, TsubataI. Preparation of barium titanate-polypyrrole compositions and their electrical properties. J Appl PolymSci 1989; 37(1): 289-293.
http://dx.doi.org/10.1002/app.1989.070370123

[3]   Shen K, Huang HT, Tseung ACC. A Study of Tungsten Trioxide and Polyaniline Composite Films I. Electrochemical and Electrochromic Behavior. J ElectrochemSoc 1992; 139(7): 1840-184.
http://dx.doi.org/10.1149/1.2069508

[4]   Peng X, Zhang Y, Yang J, Zou B, Xia PL, Li T, Yang J. Formation of nanoparticulate iron (III) oxide-stearate multilayer through Langmuir-Blodgett method. J PhysChem 1992; 96(8): 3412-3415.
http://dx.doi.org/10.1021/j100187a043

[5]   Wang W, Sarang PG, Jiao Q, Zhao B. Ferrite-grafted polyaniline nanofibers as electromagnetic shielding materials. J Mat Chem C2013; 1(16): 2851-2859.
http://dx.doi.org/10.1039/c3tc00757j

[6]   Saini P, Choudhary V, Dhawan SK. Improved microwave absorption and electrostatic charge dissipation efficiencies of conducting polymer grafted fabrics prepared via in situ polymerization. Polym Advan Technol 2012; 23(3): 343-349.
http://dx.doi.org/10.1002/pat.1873

[7]   Wan M, Zhou W, Li J. Composite of polyaniline containing iron oxides with nanometer size. Synt Met 1996; 78: 27-31.
http://dx.doi.org/10.1016/0379-6779(95)03562-1

[8]   Aphesteguy JC, Jacobo SE. Composite of polyaniline containing iron oxides. Physica B 2004; 354: 224-227.
http://dx.doi.org/10.1016/j.physb.2004.09.053

[9]   Xia H, Cheng D, Xiao C, Chan HSO.Controlled synthesis of polyaniline nanostructures with junctions usingin situself-assembly of magnetic nanoparticles. J Mat Chem2005; 15: 4161-4166.
http://dx.doi.org/10.1039/b508629a

[10]   Araújo ACV, de Oliveira RJ, Alves JS, Rodrigues AR, Machado FLA, Cabral FAO, de Azevedo WM. Synthesis, characterization and magnetic properties of polyaniline-magnetite nanocomposites. Synthetic Met 2010: 160: 685-690.
http://dx.doi.org/10.1016/j.synthmet.2010.01.002

[11]   Della Pina C, Falletta E. Gold-catalyzed oxidation in organic synthesis: a promise kept. Catal Sci Technol 2011; 1: 1564-71.
http://dx.doi.org/10.1039/c1cy00283j

[12] Della Pina C, Falletta E, Rossi M. Update on selective oxidation using gold. ChemSoc Rev 2012; 41: 350-69.
http://dx.doi.org/10.1039/C1CS15089H

[13] Comotti M, Della Pina C, Matarrese R, Rossi M. The Catalytic Activity of "Naked" Gold Particles. Angew ChemInt Ed 2004; 43: 5812-5.
http://dx.doi.org/10.1002/anie.200460446

[14] Chen Z, Della Pina C, Falletta E, *et al*. Facile synthesis of polyanilineusinggoldcatalyst. J Catal 2008; 259: 1-4.
http://dx.doi.org/10.1016/j.jcat.2008.07.006

[15] Della Pina C, Falletta E, Lo Faro M, Pasta M, Rossi M. Gold-catalysed synthesis of polypyrrole**.** Gold Bull 2009; 42: 27-33.
http://dx.doi.org/10.1007/BF03214903

[16] Chen Z, Della Pina C, Falletta E, Rossi M. A green route to conducting polyaniline by copper catalysis. J Catal 2009; 267: 93-6.
http://dx.doi.org/10.1016/j.jcat.2009.07.007

[17] Della Pina C, Rossi M, Ferretti AM, Ponti A, Lo Faro M, Falletta E. One-pot synthesis of polyaniline/Fe_3O_4nanocomposites with magnetic and conductive behaviour. Catalytic effect of Fe_3O_4 nanoparticles. Synth Met 2012; 162: 2250-8.
http://dx.doi.org/10.1016/j.synthmet.2012.10.023

[18] Della Pina C, Ferretti AM, Ponti A, Falletta E. A green approach to magnetically-hard electrically-conducting polyaniline/$CoFe_2O_4$ nanocomposites. Compos Sci Technol 2015; 110: 138-144.
http://dx.doi.org/10.1016/j.compscitech.2015.02.007

[19] Fabian K. Approach to saturation analysis of hysteresis measurements in rock magnetism and evidence for stress dominated magnetic anisotropy in young mid-ocean ridge basalt. Phys Earth Planet Inter 2006; 154: 299-307.
http://dx.doi.org/10.1016/j.pepi.2005.06.016

[20] Zhao SY, Lee DK, Kim CW, Cha HG, Kim YH, Kang YS. Synthesis of Magnetic Nanoparticles of $Fe_3O_4$and $CoFe_2O_4$and Their Surface Modification by Surfactant Adsorption. Bull Korean Chem Soc 2006; 27(2): 237-242.
http://dx.doi.org/10.5012/bkcs.2006.27.2.237

[21] Wang H, Huang J, Ding LY, Wang C, Han Y. Controlled preparation ofmonodisperse $CoFe_2O_4$ nanoparticles by a facile method. J Wuhan Univ Technol - Mater Sci Ed 2011; 26(2): 258-62.
http://dx.doi.org/10.1007/s11595-011-0209-1

[22] Deraz NM, Abd-Elkader OH. Investigation of Magnesium Ferrite Spinel Solid Solution with Iron-Rich Composition. Int J Electrochem Sci 2013; 8: 9071 - 9081.

[23] Bangale SV, Patil DR, Bamane SR. Preparation and electrical properties of nanocrystalline $MgFe_2O_4$ oxide by combustion route. ArchAppl Sci Res 2011; 3(5):506-513.

[24] Omer MIM, Elbadawi AA, Yassin OA. Synthesis and Structural Properties of $MgFe_2O_4$ Ferrite Nano-particles. J ApplIndSci 2013; 1(4): 2328-4609.

[25] Della PinaC, FallettaE, RossiM.Conductive materials by metal catalyzed polymerization. Cat Today 2011; 160: 11-27.
http://dx.doi.org/10.1016/j.cattod.2010.05.023

[26] Wei Y, Jang GW, Chan CC, Hsuen KF, Hariharan R, Patel SA, Whitecar CK. Polymerization of aniline and alkyl ring-substituted anilines in the presence of aromatic additives. J PhysChem 1994; 94: 7716-7721.
http://dx.doi.org/10.1021/j100382a073

[27] Wei Y, Tang X, Sun Y. Focke WW. A study of the mechanism of aniline polymerization. J PolymSci 1989; 27: 2385-2396.
http://dx.doi.org/10.1002/pola.1989.080270720

[28] CAS Number 101-54-2.

[29] Zhonga Y, Liang X, He Z, Tana W, Zhua J, Yuan P, Zhu R, He H. The constraints of transition metal substitutions (Ti, Cr, Mn, Co and Ni) in magnetite on its catalytic activity in heterogeneous Fentonand UV/Fenton reaction: From the perspective of hydroxylradical generation. Appl Catal B2014; 612- 61: 8150- 151.

[30] Sun ZC, Geng YH, Li J, Wang XH, Jing XB, Wang FS. Catalytic oxidization polymerization of aniline in an H_2O_2-Fe^{2+}system. J ApplPolymSci1999; 72:1077-1084.
http://dx.doi.org/10.1002/(SICI)1097-4628(19990523)72:8<1077::AID-APP12>3.0.CO;2-V

[31] Sun ZC, Geng YH, Li J, Jing XB, Wang FS. Chemical polymerization of aniline with hydrogen peroxide as oxidant. Synthetic Met1997; 84: 99-100.
http://dx.doi.org/10.1016/S0379-6779(96)03855-6

[32] Svoboda J, Bláha M, Sedláček J, Vohlídal J, Balcar H, Mav-Goležl, ŽigonM. New Approaches to the Synthesis of Pure Conjugated Polymers.ActaChimSlov2006; 53: 407-416.

[33] Salaneck WR, Liedberg B, Inganas O, Enandsson R, Lundstrom L, MacDiarmid AG, Halpem M, Somasin NLD. Physical Characterization of Some Polyaniline, (øN)^x.MolLiqCryst 1985; 121: 191-194.
http://dx.doi.org/10.1080/00268948508074860

[34] Tauxe L, Mullender TAT, Pick T. Potbellies, wasp-waists, and superparamagnetism in magnetic hysteresis. J Geophys Res - Solid Earth 1996; 101: 571-83.
http://dx.doi.org/10.1029/95JB03041

[35] Cullity BD, Graham CD. Introduction to magnetic materials. 2nd ed. IEEE Press-Wiley 2009.

[36] Batlle X, Labarta A. Finite-size effects in fine particles: magnetic and transport properties. J Phys D – Appl Phys 2002; 35: R15-42.

[37] Stejskal J, Gilbert RG. Polyaniline. Preparation of a conducting polymer (IUPAC technical report). Pure Appl Chem 2002; 74(5): 857-67.
http://dx.doi.org/10.1351/pac200274050857

[38] Della PinaC, FallettaE, Polyaniline from tradition to innovation, ISBN: 978-1-63463-273-7, Nova Science Publishers, Inc. New York 2015.

[39] Della Pina C, Zappa E, Busca G, Falletta E. Electromechanical properties of polyanilines prepared by twodifferent approaches and their applicability in force measurements. Sens & Act B 2014;201: 395-401.
http://dx.doi.org/10.1016/j.snb.2014.04.105

[40] Falletta E, Costa P, Della Pina C, Lanceros-Mendez S. Development of high sensitive polyaniline based piezoresistive filmsby conventional and green chemistry approaches. Sens & Act B A 2014; 220: 13-21.
http://dx.doi.org/10.1016/j.sna.2014.09.004